


ARTICLE

Open Access



# Effect of halogens on 3-[4-(dimethylamino)phenyl]-1-phenylprop-2-en-1-ones: development of a new class of monoamine oxidase-B inhibitors

Haydara Ammar Hasan<sup>1†</sup>, Jiseong Lee<sup>2†</sup>, Sunil Kumar<sup>1</sup>, Saleh Alfarraj<sup>3</sup>, Sulaiman Ali Alharbi<sup>4</sup>, Manu Pant<sup>5</sup>, Hoon Kim<sup>2\*</sup>  and Bijo Mathew<sup>1\*</sup>

## Abstract

Five dimethylamino-based chalcone derivatives (AC) were synthesized and evaluated for their inhibition degree against monoamine oxidase (MAO) enzymes. All AC compounds showed better inhibitory activity against MAO-B than that against MAO-A. AC4 showed the highest inhibitory ability with an  $IC_{50}$  value of 0.020  $\mu$ M, similar to that of a reference drug safinamide ( $IC_{50}$ =0.019  $\mu$ M) against MAO-B, followed by AC1 ( $IC_{50}$ =0.068  $\mu$ M) and AC3 ( $IC_{50}$ =0.083  $\mu$ M). Substituent -F in ring A (AC4) increased the MAO-B inhibition, followed by -H (AC1), -Br (AC3), and -Cl (AC2). The selectivity index (SI) value of AC4 was high (SI=82.00) as well as other compounds (44.41 to 98.15). AC4 was found to be a reversible inhibitor as confirmed through analysis using the dialysis method. Interestingly, AC4 was observed to be a noncompetitive MAO-B inhibitor with a rare case and with  $K_i$  values of  $0.011 \pm 0.0036$   $\mu$ M. These experiments confirmed that AC4 is a reversible and potent selective inhibitor of MAO-B. Molecular docking experiments revealed that AC4 showed the highest inhibitory activity with a docking score (-9.510 kcal/mol). A study using molecular dynamics modeling revealed that the protein–ligand complex was more stable. It was observed that AC4 was non-cytotoxic in the study using L929 cell line. In conclusion, compound AC4 shows promise as a MAO-B inhibitor.

**Keywords** Dimethylamine chalcones, Monoamine oxidase-B, Kinetics, Swiss target prediction, Molecular dynamics

<sup>†</sup>Haydara Ammar Hasan and Jiseong Lee contributed equally to this work.

\*Correspondence:

Hoon Kim

hoon@sunchon.ac.kr

Bijo Mathew

bijomathew@aims.amrita.edu; bijovilaventgu@gmail.com

<sup>1</sup>Department of Pharmaceutical Chemistry, Amrita School of Pharmacy, Amrita Vishwa Vidyapeetham, AIMS Health Sciences Campus, Kochi 682 041, India

<sup>2</sup>Department of Pharmacy, and Research Institute of Life Pharmaceutical Sciences, Sunchon National University, Suncheon 57922, Republic of Korea

<sup>3</sup>Zoology Department, College of Science, King Saud University, Riyadh 11451, Saudi Arabia

<sup>4</sup>Department of Botany, College of Science, King Saud University, Riyadh 11451, Saudi Arabia

<sup>5</sup>School of Pharmacy, Graphic Era Hill University, Dehradun 248002, India

## Introduction

The mitochondrial-bound enzymes known as monoamine oxidases (MAOs) catalyze the oxidative deamination of biogenic amines. They play a pivotal role in the metabolism of hormones, dietary amines (*p*-tyramine), and potentially harmful exogenous amines such as 1-methyl-4-phenyl-1,2,3,6-tetrahydropyridine [1, 2]. MAO enzymes are classified into two isoforms, i.e., MAO-A and MAO-B, based on their tissue distribution, and inhibitor and substrate discrimination. In the case of MAO-B, the preferred substrates are tiny exogenous amines, i.e., like benzylamine and phenethylamine. It is mainly found in the hypothalamus, sites rich in dopamine (DA) neurons, and selectively metabolizes bulky endogenous amines such as 5-hydroxytryptamine and noradrenaline. It is primarily expressed in the catecholaminergic neurons [3–6]. This makes human MAO-A and MAO-B targets for the treatment of major depressive disorders, anxiety, refractory depression, atypical depression, and neurodegenerative diseases [7–9].

Specifically, it has been shown that blocking MAO-B provides neuroprotection by reducing the reactive oxygen species generation, stabilizing the mitochondrial membrane, and promoting anti-apoptotic processes [10–12]. Furthermore, it is known that as people age, brain MAO-B activity increases and is typically higher than normal. It is directly linked to cognitive decline, affected by neurodegenerative illnesses, like as Parkinson's disease (PD) and Alzheimer's disease (AD) and neurodegeneration [13–15]. Currently, MAO-B inhibitors are regarded as viable substitutes for L-DOPA and DA agonists during the first-line therapy of PD, but medical chemists still face challenges in finding strong and specific inhibitors [16, 17].

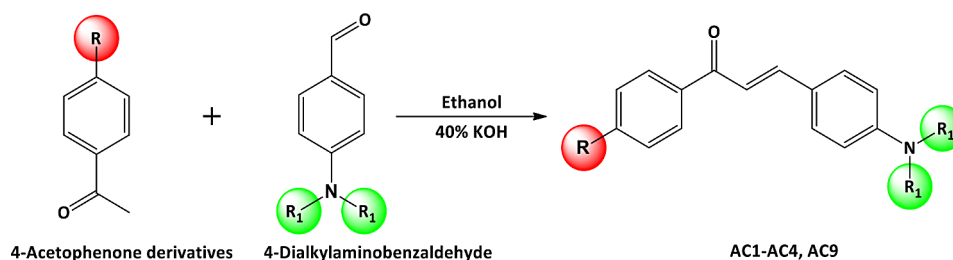
Recently, various chalcone compounds have been studied to create reversible and highly selective MAO inhibitors [18]. These molecules are open chain flavonoids (1,3-diphenyl-2-propenones) and are made up of two aryl rings that are separated by an unsaturated carbonyl linker ( $\alpha$ ,  $\beta$ ). Additionally, the data point to the possibility that coplanarity between the neighboring conjugated ketone and the A ring in chalcones could promote MAO-B inhibition [19–21]. Furthermore, it has been found that multimodal inhibitors of MAO-B and acetylcholinesterase (AChE) maintain the specific inhibitory characteristics of chalcones on MAO-B [22–24].

Moreover, the use of 4-dimethylamino chalcone derivatives has been gaining increasing attention due to its importance in inhibiting MAO-A, MAO-B, and AChE [25–27]. Additionally, current research indicates that 4-dimethylamino chalcone derivatives are being studied extensively as imaging probes for  $\text{A}\beta$  aggregates; it appears that the dimethylamino group contributes to the significant binding affinity to  $\text{A}\beta$  aggregates [28–30]. By combining the two pharmacophores, a novel series of diethylamino and chalcone derivatives was created to investigate their structure-activity relationship in more detail.

## Materials and methods

### Synthesis

A solution of ethanol (10 mL) and 40% potassium hydroxide (5 mL) was stirred for 5 min using a magnetic stirrer. Equimolar amounts of the substituted acetophenone derivatives were dissolved in 5 mL ethanol with stirring, and 15 mL ethanolic KOH was added to this solution (Scheme 1). The solution was stirred for 5 min and equimolar of 4-dialkylamino benzaldehyde respectively, were



CODE	R	R <sub>1</sub>
AC1	H	CH <sub>3</sub>
AC2	Cl	CH <sub>3</sub>
AC3	Br	CH <sub>3</sub>
AC4	F	CH <sub>3</sub>
AC9	Cl	C <sub>2</sub> H <sub>5</sub>

**Scheme 1** Synthesis of the AC derivatives

added. Then, the mixture was stirred continuously for 2 h until a precipitate formed. After filtering and washing the mixture with ethanol and distilled water, methanol was recrystallized. All compounds were characterized by using  $^1\text{H}$  NMR and  $^{13}\text{C}$  NMR spectra and yields were mentioned in Supplementary Information [Figs. S1 – S5].

#### Enzyme assays and kinetics

Enzyme assays were carried out by continuous method and kynuramine and benzylamine were used as substrates for MAO-A and MAO-B, respectively [24]. The concentrations used were 0.06 and 0.3 mM, respectively. For enzyme kinetics, activity was analyzed at five substrate concentrations near the  $K_m$  value, as determined by preliminary experiments.

#### Inhibition studies of MAO-A and MAO-B

Residual activities for MAO-A and MAO-B were preliminarily analyzed at 10 and 1  $\mu\text{M}$ , respectively, and then,  $\text{IC}_{50}$  values were determined [31]. The upper limit of  $\text{IC}_{50}$  was 40  $\mu\text{M}$ . The selectivity index (SI) for MAO-B over MAO-A was calculated by their  $\text{IC}_{50}$  values [32]. The inhibition type of AC4 for MAO-B was analyzed at three inhibitor concentrations around its  $\text{IC}_{50}$  value as well as five substrate concentrations around the  $K_m$  value [33]. Its inhibition type and  $K_i$  value were determined by using Lineweaver-Burk (LB) and its secondary plot, respectively [34].

#### Reversibility studies

The reversibility of AC4 was analyzed by dialysis method, including the pre-incubation of MAO-B and an inhibitor for 30 min prior to measurement, residual activities were measured for the undialyzed ( $A_U$ ) and dialyzed ( $A_D$ ) steps at approximately 2 x the  $\text{IC}_{50}$ . Reference MAO-B inhibitors used were safinamide mesylate as the reversible inhibitor and pargyline as the irreversible inhibitor [35].

#### SwissTarget prediction

A free web-based tool called SwissTarget prediction ([www.swisstargetprediction.ch](http://www.swisstargetprediction.ch)) was used to forecast targets for the chemical structure [36].

#### Swiss ADME

The Swiss Institute of Bioinformatics (SIB) created the web tool Swiss ADME (<https://www.swissadme.ch/>), which enables scientists to predict the pharmacokinetics, and drug-likeness of small compounds. This is a helpful tool for assessing potential drug candidates during drug development and discovery [37, 38].

#### Molecular docking studies

The hMAO-B structure (entry code 2V5Z) was retrieved from the PDB RCSB database. Maestro's

Protein Preparation Wizard preprocesses the crystal 3D structure by addressing bond ordering, eliminating unnecessary elements, and modifying structural issues, such as the absence of atoms, loops, or side chains [39, 40]. The 2D structures of AC1, AC2, AC3, and AC4 as well as low-energy 3D adherents with correct bond lengths and angles were discovered. The potential ionization states for every ligand structure were produced assuming a physiological pH of  $7.2 \pm 0.2$ . Docking was completed using the Glide module of the Schrödinger and all other parameters were maintained at their factory default values [41, 42].

#### Molecular dynamics (MD) studies

By using the Desmond MD simulation program possessing a minimum of negative score and highest docking poses, MD was carried out by running a 100-ns MD simulation to learn more about the interactions between MAO-B and AC4 [43–45]. Specifically, 100 ns of MD generation was carried out to produce trajectories of 1000 frames each [46–48]. The Root Mean Square Deviation (RMSD) and Root Mean Square Fluctuation (RMSF) were calculated for every frame. Subsequently, a stability study was conducted using a simulated interaction diagram.

#### Cytotoxicity test of AC4 to L929 cell line

The L929 (Mouse Fibroblast cell line) was provided by the National Center for Cell Science (NCCS), Pune, India. The detailed protocol was explained in Supporting Information.

## Results and discussion

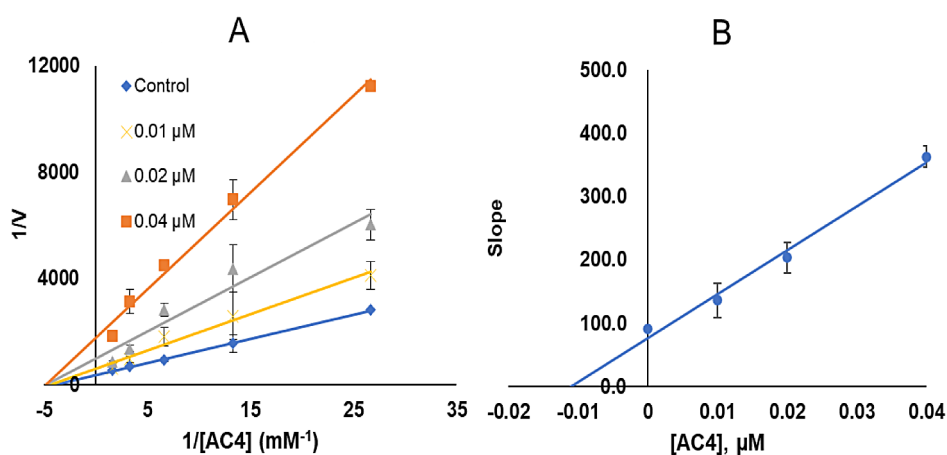
#### Inhibition studies of MAO-A and MAO-B

All tested compounds exhibited low residual activity of less than 50% for MAO-B at 1  $\mu\text{M}$ , while three compounds showed low residual activity (<50%) for MAO-A at 10  $\mu\text{M}$  (Table 1). Compound AC4 had an  $\text{IC}_{50}$  value of 0.020  $\mu\text{M}$ , showing the highest inhibitory activity against MAO-B, followed by AC1 ( $\text{IC}_{50}=0.068$   $\mu\text{M}$ ) and AC3 ( $\text{IC}_{50}=0.083$   $\mu\text{M}$ ). The best MAO-A inhibitor was AC4 with an  $\text{IC}_{50}$  of 1.64  $\mu\text{M}$ . All compounds showed more effective MAO-B inhibition than MAO-A inhibition, with high SI values for MAO-B, i.e., AC2 with 98.15, followed by AC3 (88.43) and AC4 (82.00). Comparing to the MAO-B reference inhibitors, AC4 had similar potency to safinamide ( $\text{IC}_{50}=0.019$   $\mu\text{M}$ ), and AC1 and AC3 showed better potency than pargyline. Especially, AC4 showed better or comparable inhibitory activity to other MAO-B reference inhibitors, such as lazabemide ( $\text{IC}_{50}=0.11$   $\mu\text{M}$ ) [49], rasagiline ( $\text{IC}_{50}=0.028 \sim 0.068$   $\mu\text{M}$ ) [50, 51], and selegiline ( $\text{IC}_{50}=0.010$   $\mu\text{M}$ ) [52].

**Table 1** Inhibition of MAO-A and MAO-B by dimethylamino-based chalcone derivatives

Compound ID	Residual activity (%)		IC <sub>50</sub> (μM)		SI
	MAO-A (10 μM)	MAO-B (1 μM)	MAO-A	MAO-B	
AC1	31.48±2.62	0.71±5.57	3.020±0.94	0.068±0.013	44.41
AC2	71.96±6.89	20.14±1.11	19.63±5.44	0.20±0.037	98.15
AC3	45.32±5.073	23.54±2.88	7.34±2.94	0.083±0.0092	88.43
AC4	15.50±2.23	-2.15±3.04	1.64±0.30	0.020±0.0030	82.00
AC9	52.42±1.14	18.41±1.92	11.37±0.41	0.23±0.047	49.43
Toloxatone	-	-	1.65±0.094	>40	0.041
Safinamide	-	-	>40	0.019±0.0019	2105.26
Clorgyline	-	-	0.008±0.001	2.43±0.71	0.0033
Pargyline	-	-	2.15±0.23	0.11±0.01	19.55

Results are the means±standard errors of duplicate or triplicate experiments

**Fig. 1** Lineweaver–Burke plots for MAO-B inhibition by AC4 (A), and the secondary plots (B) of the slopes vs. inhibitor concentrations

All AC compounds are chalcone-based derivatives, with an N, N-dialkyl group bonded to the B-ring and a halogen bonded to the para position of ring A. Although the IC<sub>50</sub> values of AC1–AC4, containing an N, N-dimethyl group in ring B, were not significantly different, substituent -F in ring A (AC4) increased MAO-B inhibition degree, followed by -H (AC1), -Br (AC3), and -Cl (AC2). In the case of AC2, IC<sub>50</sub> value was similar to that of AC9, containing an N, N-diethyl group instead of an N, N-dimethyl group.

#### Inhibition kinetics

After performing inhibition kinetics at five benzylamine concentrations and three AC4 concentrations, LB plot was constructed. In the plot, the lines met a point on X-axis, suggesting AC4 is a noncompetitive MAO-B inhibitor (Fig. 1A), and in the secondary plot, K<sub>i</sub> value was calculated to be 0.011±0.0036 μM, indicating it is a potent MAO-B inhibitor (Fig. 1B). Regarding inhibition types, most MAO-B inhibitors have been known to be competitive. Only a few noncompetitive MAO-B inhibitors were reported; 4-(O-benzylphenoxy)-N-methylbutylamine showed

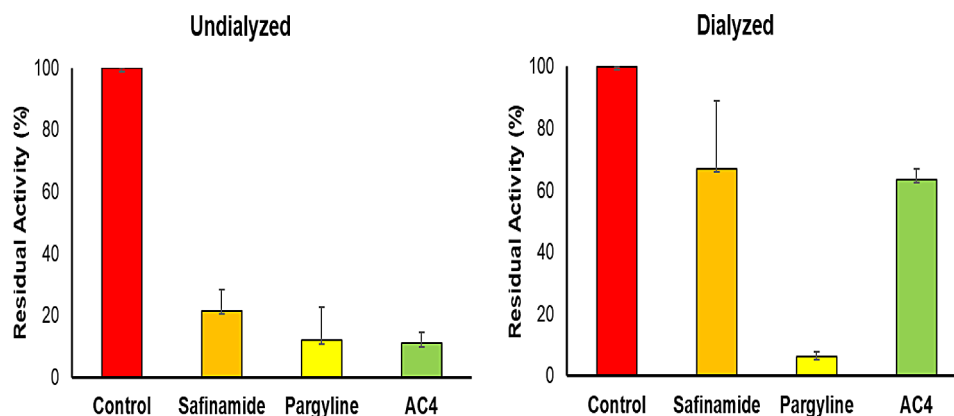
noncompetitive MAO-B inhibition; however, it had a much higher affinity for MAO-A and was more potent against MAO-A than MAO-B [53]. Curcumin inhibited MAO-B in a noncompetitive manner [54].

#### Reversibility studies

For the reversibility test of MAO-B inhibition by AC4, dialysis method was used involving 30 min of pre-incubation. Recovery patterns were considered by using undialyzed (A<sub>U</sub>) and dialyzed (A<sub>D</sub>) relative activities. In the results, inhibition of MAO-B by AC4 was recovered from 10.94 to 63.51%. The values of AC4 were similar those of safinamide (reversible type, from 21.50 to 66.95%) and it was distinguished from those of pargyline (irreversible type, 11.92–6.36%). These results suggested that AC4 is a reversible type MAO-B inhibitor (Fig. 2).

#### SwissTarget prediction

Determining the correct molecular target for a given scaffold can be difficult, with many drug design attempts. Recently, ligand-based target prediction using SwissTarget Prediction ([www.swisstargetprediction.ch](http://www.swisstargetprediction.ch)), an online





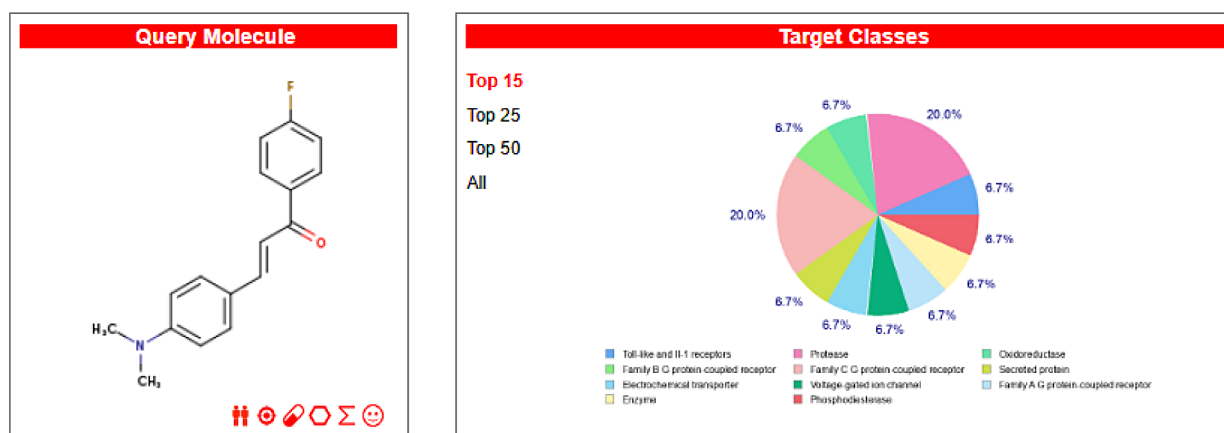


**Fig. 2** Reversibility test of MAO-B inhibition by AC4 using dialysis experiments. The concentrations of AC4, safinamide, and pargyline used were 0.040, 0.038, and 0.22  $\mu$ M, respectively ( $\sim 2 \times$  their  $IC_{50}$  values)



Export results:    

Show  entries

Search:

Target	Common name	Uniprot ID	ChEMBL ID	Target Class	Probability*	Known actives (3D/2D)
Toll-like receptor (TLR7/TLR9)	TLR9	Q9NR96	CHEMBL5804	Toll-like and Il-1 receptors	<div style="width: 100%; height: 10px; background-color: green;"></div>	14 / 4 
Cathepsin L	CTSL	P07711	CHEMBL3837	Protease	<div style="width: 100%; height: 10px; background-color: green;"></div>	63 / 3 
Monoamine oxidase B	MAOB	P27338	CHEMBL2039	Oxidoreductase	<div style="width: 100%; height: 10px; background-color: green;"></div>	311 / 62 
Cathepsin (V and K)	CTSV	O60911	CHEMBL3272	Protease	<div style="width: 100%; height: 10px; background-color: green;"></div>	9 / 0 

**Fig. 3** SwissTarget Prediction of compound AC4

tool, was used to find comparable molecules among 376,342 compounds, which are already known to be active toward 3068 macromolecular targets experimentally [36]. Figure 3 presents the prediction for the AC4 compound, which shows that the molecule has a good chance of striking a specific hMAO-B target.

### Swiss ADME

For a molecule to be regarded as an effective drug, it must demonstrate significant biological activity at low therapeutic concentrations, have minimal toxicity, and remain effective until the desired outcome is achieved. During drug discovery, the ADME properties of potential drugs are considered to provide

a superior pharmacokinetic profile. using the Swiss ADME database and pkCSM [37, 38]. In silico predictions of pharmacokinetic parameters were made. Intestinal permeability and dissolution were measured to evaluate drug absorption. The logarithm of molar concentration was used to express the proposed molecule's solubility, which ranged from  $-3.84$  to  $-6.06$  in an aqueous system. To achieve enhanced permeability, the  $P_{app}$  value of the compound must be greater than  $8 \times 10^{-6}$  cm/s. However, AC4 exhibited significant gastrointestinal absorption (96.5%). The drug distribution profile was estimated using the volume of distribution (VDss), unbound fraction, and blood-brain barrier (BBB) permeability. The log VDss was 0.245, indicating a wider distribution of the medication in the tissues than in the plasma. The fraction-bound method of measuring drug effectiveness indicates that the drug is less bound to blood proteins, and may thus be distributed freely. Swiss ADME and pkSCM were used to assess BBB permeability. With a log BB value of 0.508, the lead chemical AC4 appears to be readily able to pass through the BBB (Table 2). Compounds with log BB values of one were found to be poorly distributed in the brain. Molecules having a log PS  $> -2$  are assumed to be penetrable to the central nervous system, while those with a log PS  $< -3$  are considered useless. In this study, AC4 penetrated the central nervous system (CNS) and inhibited CYP1A2, CYP2C19, and CYP2D6. This investigation also showed that AC4 had an overall clearance rate of 0.324 log mL/min/kg. It is a strong candidate owing to its advantageous ADME features.

### Molecular docking

Compounds AC1-AC4 were used in the docking investigations because of their strong activity. The molecular interactions of the chemicals with MAO-B and their in-silico ability to block the enzyme were assessed in silico. The compound AC4 was the most active with docking score  $-9.510$  kcal/mol (Table 2). The van der Waals interactions with the hydrophobic regions surrounded by TYR60, PHE99, PRO102, PHE103, PRO104, TRP119, LEU164, LEU167, PHE168, LEU171, CYS172, ILE198, ILE199, GLN206, ILE316, TYR326, LEU328, PHE343, TYR398, and TYR435 were based on the docking position of

hMAO-B (Fig. 4). Additionally, as demonstrated in the 3D docking pose, the fluoroacetophenone ring forms a sandwich between amino acids PHE343 and TYR435 and binds to the substrate cavity (close to FAD). However, as shown in Fig. 4, the dimethylaminobenzaldehyde group was bound to the entrance cavity. Overall, our results suggest that AC4 inhibits the enzymatic activity of MAO-B.

### Molecular dynamics

A brief image of the interaction between a protein and ligand was generated through molecular docking, where molecular interactions are dynamic networks that underpin all biological systems. To examine the different conformations, we used an explicit water model to mimic the dynamic behavior of the AC4-hMAO-B docked complex during a 100 ns time span. The main objectives were to maintain the ligand in the substrate-binding pocket of the hMAO-B enzyme and preserve the important connections observed in the optimally docked posture during the MD simulation. The hMAO-B with AC4 RMSD of hMAO-B ranged from 0.9 to 4.2 Å. The average RMSD value of the complex was around 2.407 Å. One fluctuation in the simulation trajectory was observed in the ligand RMSD at 18–52 ns intervals, which progressively converged for the remainder of the analysis (Fig. 5A). The RMSF of a protein is frequently used in addition to the RMSD to assess ligand-induced changes in a protein's internal chains. The flexible area of the protein was described in depth using protein RMSF plot analysis. A high RMSF value indicates flexibility, whereas a low RMSF value indicates rigidity of the amino acid [45, 55]. According to the RMSF plot, AC4 came into touch with 18 amino acids of the hMAO-B protein, particularly, LEU88 (0.749 Å), PHE99 (0.976 Å), PRO104 (0.875 Å), TRP119 (0.804 Å), LEU164 (0.652 Å), LEU167 (0.683 Å), PHE168 (0.648 Å), LEU171 (0.761 Å), CYS172 (0.613 Å), TYR188 (0.512 Å), ILE198 (0.573 Å), ILE199 (0.698 Å), ILE316 (0.668 Å), TYR326 (0.648 Å), LEU328 (0.734 Å), PHE343 (0.552 Å), TYR398 (0.523 Å), and TYR435 (0.461 Å). All interacting residues in the AC4-hMAO-B complex exhibited RMSF values of less than 1 Å, suggesting that the residue's conformation kept stable during the simulation (Fig. 5B). As shown by the Interaction pattern of AC4 with hMAO-B, AC4 showed a variety of interactions with different substrates in the binding sites during the simulation. Pi-Pi stacking bonds were present in both benzene rings, with TYR 326 and TYR 398 comprising 43% and 68% of them, respectively. In addition, the oxygen in the ketone group formed a hydrogen bond with CYS172 having 76% (Fig. 5C). The hydrophobic amino acids interacting with AC4, LEU88, PHE99,

**Table 2** Docking scores of AC1-AC4 with hMAO-B protein structure

Compound	Docking score (kcal/mol)
AC1	-9.492
AC2	-9.467
AC3	-9.308
AC4	-9.510

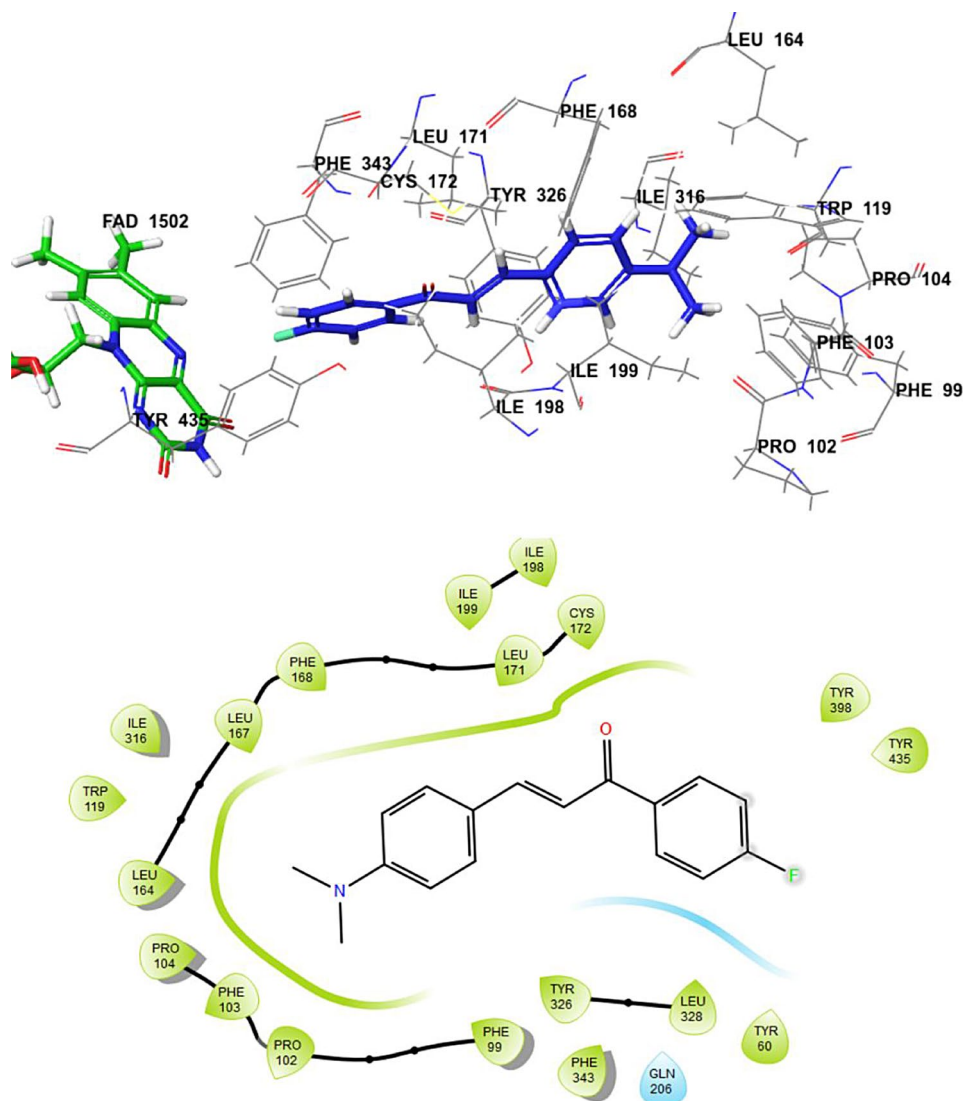


**Fig. 4** Binding interactions of AC4 to the hMAO-B active site (PDB ID: 2V5Z)

PRO104, TRP119, LEU164, LEU167, PHE168, LEU171, ILE198, ILE199, ILE316, TYR326, LEU328, PHE343, TYR398, and TYR435 were identified (Fig. 5D).

#### Effect of AC4 on cell viability in L929

Constant and fibroblast-like, the L929 cell line was isolated from the subcutaneous connective tissue of mice (*Mus musculus*). Because of their sensitivity, L929 cells are often used to evaluate the cytotoxicity of a variety of compounds, including chemicals, drugs, and biomaterials. Given that there was no discernible decrease (100  $\mu\text{g}/\text{mL}$  with 90% cell viability) in any of the test sample concentrations, the provided sample can be regarded as non-cytotoxic to normal cells (Fig. 6). The fundamental morphological changes in the cells at each dose were observed under a microscope (Fig. S6).

Collectively, the efficacy of five chalcone derivatives (AC) based on the ability of the dimethylamino group in inhibiting MAOs was evaluated. All AC compounds showed better inhibition degree against MAO-B than against MAO-A. AC4 is a selective MAO-B inhibitor with noncompetitive and reversible modes of action. The fluoro-acetophenone ring was found to be bound near FAD through docking investigations and was positioned between TYR435 and PHE343. In a simulation study, it was found that hydrophobic interactions (48–68%) and hydrogen bonding (76%) contributed to the stability of the AC4-MAO-B complex. These findings imply that AC4 may be used as a medicinal drug to treat neurological conditions such as PD.

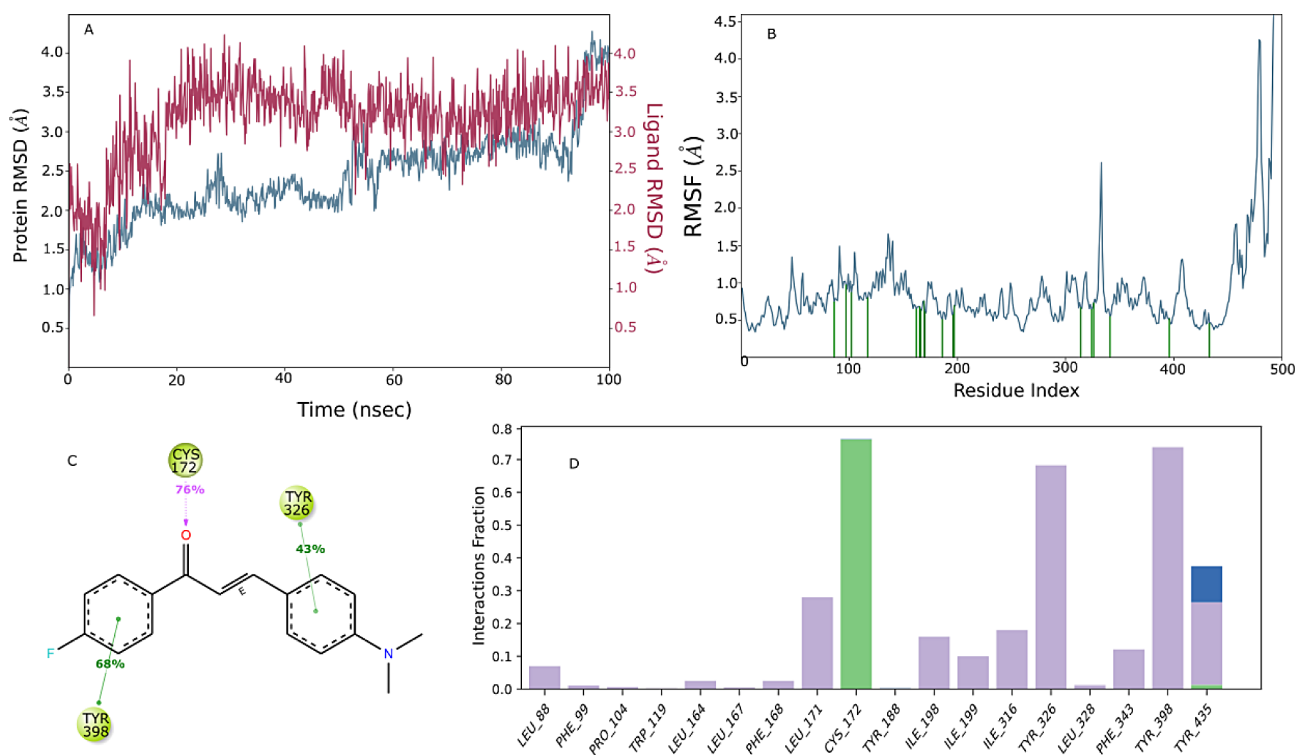


**Fig. 5** MD simulation of the AC4-MAO-B complex for RMSD (A), RMSF (B), 2D interaction diagram (C), and protein – ligand interaction analysis of the MD trajectory (D)

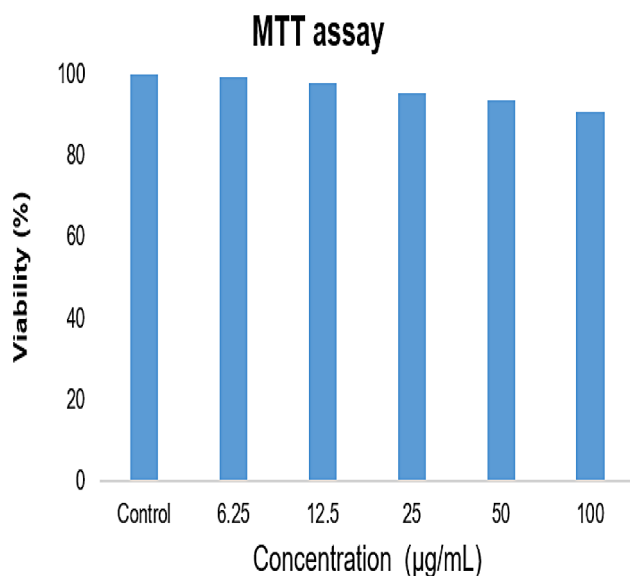


**Fig. 6** The cell viability of AC4 on L929 cell line analyzed by MTT assay. X axis, concentration of AC4; Y axis, % viability

### Supplementary Information

The online version contains supplementary material available at <https://doi.org/10.1186/s13765-024-00929-z>.

Supplementary Material 1

### Acknowledgements

The authors extend their appreciation to the Researchers Supporting Project Number (RSP2025R7) in King Saud University, Riyadh, Saudi Arabia.

### Author contributions

Conceptualization, BM and HK; synthesis, HAH, SA, SAA and SK; biological tests, JL; docking simulation and ADMET study, SK, MP, SA, and SAA.; writing—original draft preparation, HAH, SK, and BM; writing—review and editing, BM and HK; supervision, BM and HK; funding acquisition, SA, SAA and HK. All authors have read and agreed to the published version of the manuscript.

### Funding

This study was supported by the Researchers Supporting Project Number (RSP2025R7) in King Saud University, Riyadh, Saudi Arabia.

### Data availability

All data generated or analyzed during the present study are included in this published article.

### Declarations

#### Competing interests

The authors declare that they have no competing interests.

Received: 18 June 2024 / Accepted: 8 August 2024

Published online: 23 August 2024

### References

- Carradori S, D'Ascenzio M, Chimenti P, Secci D, Bolasco A, Selective MAO-B, Inhibitors (2014) A lesson from Natural products. *Mol Divers* 18(1):219–243
- Blaschko H, Richter D, Schlossmann H (1937) The inactivation of adrenaline. *J Physiol* 90(1):1–17
- Johnston JP (1968) Some observations upon a new inhibitor of Monoamine Oxidase in Brain tissue. *Biochem Pharmacol* 17(7):1285–1297



4. Murphy DL (1978) Substrate-selective Monoamine Oxidases—Inhibitor, tissue, species and functional differences. *Biochem Pharmacol* 27(15):1889–1893
5. De Colibus L, Li M, Binda C, Lustig A, Edmondson DE, Mattevi A (2005) Three-Dimensional structure of human monoamine oxidase A (MAO A): relation to the structures of Rat MAO A and Human MAO B. *Proc Natl Acad Sci U S A* 102(36):12684–12689
6. Binda C, Hubálek F, Li M, Edmondson DE, Mattevi A (2004) Crystal structure of human monoamine oxidase B, a drug target enzyme Monotopically inserted into the mitochondrial outer membrane. *FEBS Lett* 564(3):225–228
7. Bortolato M, Chen K, Shih JC (2008) Monoamine Oxidase inactivation: from pathophysiology to therapeutics. *Adv Drug Deliv Rev* 60(13–14):1527–1533
8. Davie CA (2008) A review of Parkinson's Disease. *Br Med Bull* 86(1):109–127
9. Youdim MBH, Edmondson D, Tipton KF (2006) The therapeutic potential of Monoamine Oxidase inhibitors. *Nat Rev Neurosci* 7(4):295–309
10. Mondovì B, Agrò AF (1982) Structure and function of Amine Oxidases. *Advances in Experimental Medicine and Biology*. Springer US, Boston, MA, pp 141–153
11. Andrews JM, Nemeroff CB (1994) Contemporary Management of Depression. *Am J Med* 97(6):S24–S32
12. Cesura AM, Pletscher A (1992) The New Generation of Monoamine Oxidase inhibitors. *Progress in Drug Research / Fortschritte Der Arzneimittelforschung / Progrès Des recherches pharmaceutiques*. Birkhäuser Basel, Basel, pp 171–297
13. Youdim MBH, Ben-Shachar D, Riederer P (1989) Is Parkinson's Disease A Progressive Siderosis of Substantia Nigra resulting in Iron and melanin Induced Neurodegeneration? *Acta Neurol Scand* 80:47–54
14. Carradori S, Silvestri R (2015) New frontiers in Selective Human MAO-B inhibitors: Miniperspective. *J Med Chem* 58(17):6717–6732
15. Emilsson L, Saetre P, Balciuniene J, Castensson A, Cairns N, Jazin EE (2002) Increased Monoamine Oxidase Messenger RNA expression levels in Frontal Cortex of Alzheimer's Disease patients. *Neurosci Lett* 326(1):56–60
16. Abell CW, Kwan S-W (2000) Molecular characterization of Monoamine Oxidases A and B. *Progress in Nucleic Acid Research and Molecular Biology*. Elsevier, pp 129–132
17. Elmer LW, Bertoni JM (2008) The increasing role of Monoamine oxidase type B inhibitors in Parkinson's Disease Therapy. *Expert Opin Pharmacother* 9(16):2759–2772
18. de Freitas Silva M, Dias KST, Gontijo VS, Ortiz CJ, Viegas C (2018) Jr. Multi-target Directed drugs as a Modern Approach for Drug Design towards Alzheimer's Disease: an update. *Curr Med Chem* 25(29):3491–3525
19. Zhuang C, Zhang W, Sheng C, Zhang W, Xing C, Miao Z (2017) Chalcone: A Privileged Structure in Medicinal Chemistry. *Chem. Rev.* 117(12), 7762–7810
20. Guglielmi P, Mathew B, Secci D, Carradori S, Chalcones (2020) Unearthing their therapeutic possibility as Monoamine Oxidase B inhibitors. *Eur J Med Chem* 205(112650):112650
21. Iacovino LG, Pinzi L, Facchetti G, Bortolini B, Christodoulou MS, Binda C, Rastelli G, Rimoldi I, Passarella D, Di Paolo ML (2021) Dalla Via, L. Promising Non-cytotoxic Monosubstituted Chalcones to Target Monoamine Oxidase-B. *ACS Med Chem Lett* 12(7):1151–1158
22. Kong Z, Sun D, Jiang Y, Hu Y, Design (2020) Synthesis, and evaluation of 1, 4-Benzodioxan-substituted Chalcones as selective and reversible inhibitors of human monoamine oxidase B. *J Enzyme Inhib Med Chem* 35(1):1513–1523
23. Mathew B, Haridas A, Suresh J, Mathew E, Uçar G, Jayaprakash G (2016) Monoamine Oxidase Inhibitory Action of chalcones: a Mini Review. *Cent Nerv Syst Agents Med Chem* 16(2):120–136
24. Oh JM, Rangarajan TM, Chaudhary R, Singh RP, Singh M, Singh RP, Tondo AR, Gambacorta N, Nicolotti O, Mathew B, Kim H (2020) Novel class of Chalcone Oxime Ethers as Potent Monoamine Oxidase-B and acetylcholinesterase inhibitors. *Molecules* 25(10):2356
25. Sang Z, Song Q, Cao Z, Deng Y, Tan Z, Zhang L, Design (2021) Synthesis and evaluation of Novel Dimethylamino Chalcone-O-Alkylamines derivatives as potential multifunctional agents against Alzheimer's Disease. *Eur J Med Chem* 216(113310):113310
26. Wang X-Q, Xia C-L, Chen S-B, Tan J-H, Ou T-M, Huang S-L, Li D, Gu L-Q, Huang Z-S (2015) Design, synthesis, and Biological evaluation of 2-Arylethenylquinoline derivatives as multifunctional agents for the treatment of Alzheimer's Disease. *Eur J Med Chem* 89:349–361
27. Tang J, Jila S, Luo T, Zhang B, Miao H, Feng H, Chen Z, Zhu G (2022) C3/ C3aR inhibition alleviates GMH-IVH-Induced Hydrocephalus by preventing microglia-astrocyte interactions in neonatal rats. *Neuropharmacology* 205(108927):108927
28. Fournier dit Chabert J, Marquez B, Neville L, Joucla L, Broussous S, Bouhours P, David E, Pellet-Rostaing S, Marquet B, Moreau N, Lemaire M (2007) Synthesis and evaluation of New Arylbenzo[b]thiophene and Diarylthiophene Derivatives as inhibitors of the NorA Multidrug Transporter of *Staphylococcus Aureus*. *Bioorg Med Chem* 15(13):4482–4497
29. Ono M, Watanabe R, Kawashima H, Cheng Y, Kimura H, Watanabe H, Haratake M, Saji H, Nakayama M (2009) Fluoro-Pegylated Chalcones as Positron Emission Tomography Probes for in vivo imaging of  $\beta$ -Amyloid plaques in Alzheimer's Disease. *J Med Chem* 52(20):6394–6401
30. Yang Y, Cui M, Jin B, Wang X, Li Z, Yu P, Jia J, Fu H, Jia H, Liu B (2013) 99mTc-Labeled dibenzylideneacetone derivatives as potential SPECT Probes for in vivo imaging of  $\beta$ -Amyloid plaque. *Eur J Med Chem* 64:90–98
31. Oh JM, Kang Y, Hwang JH, Park J-H, Shin W-H, Mun S-K, Lee JU, Yee S-T, Kim H (2022) Synthesis of 4-Substituted Benzyl-2-triazole-linked-tryptamine-paeonol derivatives and evaluation of their selective inhibitions against butyrylcholinesterase and Monoamine Oxidase-B. *Int J Biol Macromol* 217:910–921
32. Baek SC, Park MH, Ryu HW, Lee JP, Kang M-G, Park D, Park CM, Oh S-R, Kim H (2019) Rhamnocitrin isolated from *Prunus Padus* Var. *Seoulensis*: a potent and selective reversible inhibitor of human monoamine oxidase A. *Bioorg Chem* 83:317–325
33. Baek SC, Ryu HW, Kang M-G, Lee H, Park D, Cho M-L, Oh S-R, Kim H (2018) Selective inhibition of Monoamine Oxidase A by Chelerythrine, an Isoquinoline Alkaloid. *Bioorg Med Chem Lett* 28(14):2403–2407
34. Oh JM, Jang H-J, Kim WJ, Kang M-G, Baek SC, Lee JP, Park D, Oh S-R, Kim H (2020) Calycosin and 8-O-Methylretusin isolated from *Maackia Amurensis* as potent and selective reversible inhibitors of human monoamine Oxidase-B. *Int J Biol Macromol* 151:441–448
35. Lee HW, Ryu HW, Kang M-G, Park D, Oh S-R, Kim H (2016) Potent selective Monoamine Oxidase B inhibition by Maackiain, a Pterocarpan from the roots of *Sophora Flavescens*. *Bioorg Med Chem Lett* 26(19):4714–4719
36. Daina A, Michielin O, Zoete V, SwissTargetPrediction (2019) Updated data and new features for efficient prediction of protein targets of small molecules. *Nucleic Acids Res* 47(W1):W357–W364
37. Daina A, Michielin O, Zoete VSADME (2017) A free web Tool to Evaluate Pharmacokinetics, Drug-Likeness and Medicinal Chemistry friendliness of small molecules. *Sci Rep* 7(1)
38. Pires DEV, Blundell TL, Ascher DB (2015) PkCSM: Predicting Small-Molecule Pharmacokinetic and Toxicity properties using graph-based signatures. *J Med Chem* 58(9):4066–4072
39. Malani A, Makwana A, Monapara J, Ahmad I, Patel H, Desai N, Synthesis M, Docking (2021) DFT Study, and in Vitro Antimicrobial activity of some 4-(Biphenyl-4-yl)-1,4-dihydropyridine and 4-(Biphenyl-4-yl)pyridine derivatives. *J Biochem Mol Toxicol* 35(11)
40. Patel S, Hasan H, Umraliya D, Sanapalli BKR, Yele V (2023) Marine drugs as putative inhibitors against non-structural proteins of SARS-CoV-2: an in silico study. *J Mol Model* 29(6)
41. *Desmond*. Schrödinger. <https://www.schrodinger.com/platform/products/desmond/> (accessed 2024-06-07)
42. Bhaskar V, Kumar S, Sujathan Nair A, Gokul S, Rajappan Krishnendu P, Benny S, Amrutha CT, Manisha DS, Bhaskar V, Mary Zachariah S, Aneesh TP, Abdelgawad MA, Ghoneim MM, Pappachen LK, Nicolotti O, Mathew B (2023) *In Silico* Development of Potential InhA Inhibitors through 3D-QSAR Analysis, Virtual Screening and Molecular Dynamics. *J Biomol Struct Dyn* 1–23
43. Abdelgawad MA, Oh JM, Parambi DGT, Kumar S, Musa A, Ghoneim MM, Nayl AA, El-Ghorab AH, Ahmad I, Patel H, Kim H, Mathew B (2022) Development of bromo- and fluoro-based  $\alpha$ ,  $\beta$ -Unsaturated ketones as highly potent MAO-B inhibitors for the treatment of Parkinson's Disease. *J Mol Struct* 1266(133545):133545
44. Pawara R, Ahmad I, Nayak D, Wagh S, Wadkar A, Ansari A, Belamkar S, Surana S, Nath Kundu C, Patil C, Patel H (2021) Novel, selective Acrylamide Linked quinazolines for the treatment of double mutant EGFR-L858R/T790M non-small-cell Lung Cancer (NSCLC). *Bioorg Chem* 115(105234):105234
45. Sudevan ST, Oh JM, Abdelgawad MA, Abourehab MAS, Rangarajan TM, Kumar S, Ahmad I, Patel H, Kim H, Mathew B (2022) Introduction of Benzyloxy Pharmacophore into Aryl/Heteroaryl Chalcone Motifs as a New Class of Monoamine Oxidase B inhibitors. *Sci Rep* 12(1)
46. Radwan HA, Ahmad I, Othman IMM, Gad-Elkareem MAM, Patel H, Aouadi K, Snoussi M, Kadri A, Design (2022) Synthesis, in Vitro Anticancer and Antimicrobial evaluation, SAR Analysis, Molecular Docking and Dynamic Simulation of New Pyrazoles, Triazoles and Pyridazines Based Isoxazole. *J Mol Struct* 1264(133312):133312

47. Acar Çevik U, Celik I, Işık A, Ahmad I, Patel H, Özkay Y, Kaplançıklı ZA, Design (2023) Synthesis, molecular modeling, DFT, ADME and biological evaluation studies of some New 1,3,4-Oxadiazole linked Benzimidazoles as Anticancer agents and Aromatase inhibitors. *J Biomol Struct Dyn* 41(5):1944–1958
48. Kumar S, Oh JM, Abdelgawad MA, Abourehab MAS, Tengli AK, Singh AK, Ahmad I, Patel H, Mathew B, Kim H (2023) Development of Isopropyl-Tailed Chalcones as a new class of selective MAO-B inhibitors for the treatment of Parkinson's disorder. *ACS Omega* 8(7):6908–6917
49. Sudevan ST, Oh JM, Abdelgawad MA, Abourehab MAS, Rangarajan TM, Kumar S, Ahmad I, Patel H, Kim H, Mathew B (2022) Introduction of benzyloxy pharmacophore into aryl/heteroaryl chalcone motifs as a new class of monoamine oxidase B inhibitors. *Sci Rep* 12(1):22404
50. Tian C, Qiang X, Song Q, Cao Z, Ye C, He Y, Deng Y, Zhang L (2020) Flurbiprofen-Chalcone hybrid Mannich base derivatives as balanced multifunctional agents against Alzheimer's disease: design, synthesis and biological evaluation. *Bioorg Chem* 94:103477
51. Sang Z, Song Q, Cao Z, Deng Y, Tan Z, Zhang L (2021) Design, synthesis and evaluation of novel dimethylamino chalcone-O-alkylamines derivatives as potential multifunctional agents against Alzheimer's disease. *Eur J Med Chem* 216:113310
52. Mzezewa SC, Omoruyi SI, Zondagh LS, Malan SF, Ekpo OE, Joubert J (2021) Design, synthesis, and evaluation of 3,7-substituted coumarin derivatives as multifunctional Alzheimer's disease agents. *J Enzyme Inhib Med Chem* 36(1):1607–1621
53. Naoi M, Maruyama W, Akao Y, Yi H, Yamaoka Y (2006) Involvement of type A Monoamine Oxidase in Neurodegeneration: regulation of mitochondrial signaling leading to cell death or neuroprotection. *Oxidative stress and Neuroprotection*. Springer Vienna: Vienna, pp 67–77
54. Juvekar A, Khatri D (2016) Kinetics of inhibition of Monoamine Oxidase using Curcumin and Ellagic Acid. *Pharmacogn Mag* 12(46):116
55. Bharadwaj KK, Ahmad I, Pati S, Ghosh A, Sarkar T, Rabha B, Patel H, Baishya D, Edinur HA, Abdul Kari Z, Ahmad M, Zain MR (2022) Wan Rosli, W. I. Potent Bioactive Compounds from Seaweed Waste to Combat Cancer through Bioinformatics Investigation. *Front. Nutr.* 9

### Publisher's Note

Springer Nature remains neutral with regard to jurisdictional claims in published maps and institutional affiliations.